JOURNAL OF GEOPHYSICAL RESEARCH, VOL. 114, D17210, doi:10.1029/2008JD011618, 2009

Click Here for Full Article

Properties of the X-ray emission from rocket-triggered lightning as measured by the Thunderstorm Energetic Radiation Array (TERA)

Z. Saleh,[1] J. Dwyer,[1] J. Howard,[2] M. Uman,[2] M. Bakhtiari,[3] D. Concha,[4] M. Stapleton,[2] D. Hill,[2] C. Biagi,[2] and H. Rassoul[1]

Received 12 December 2008; revised 27 March 2009; accepted 10 June 2009; published 15 September 2009.

[1] The Thunderstorm Energetic Radiation Array (TERA) is located at the University of Florida, Florida Tech International Center for Lightning Research and Testing (ICLRT) at Camp Blanding, Florida. The array includes forty-five 7.6-cm-diameter NaI/photomultiplier tube detectors enclosed in 24 separate aluminum boxes that shield the detectors from light, moisture, and RF noise. The array covers the $\sim$1 km^2 ICLRT facility, centered on the rocket launch tower, used to trigger lightning. From 2005 to 2007, TERA recorded seven rocket-triggered lightning flashes. In this paper we present an analysis of the X-ray emission of three of these flashes. The X-ray emission is observed to occur during the dart leader phase of each stroke, just prior to the time of the return stroke. Significant X-rays are observed on all the detectors to a distance of 500 m from the lightning channel for times up to 200 μs prior to the start of the return stroke. Using Monte Carlo simulations to model the X-ray propagation, we find that the energetic electrons that emit the X-rays have a characteristic energy of about 1 MeV for one particular dart-stepped leader event. The X-ray emission for all three events has a radial fall off proportional to [exp $(-r/120)$]/r and is most consistent with the energetic source electrons being emitted isotropically from the leader. It is also found that the X-ray and energetic electron luminosities of the leader channel decreases with increasing height above the ground. These results help shed light onto the mechanism for producing energetic radiation from lightning. For instance, a characteristic energy of 1 MeV is not consistent with the relativistic runaway electron avalanche mechanism, suggesting that so-called cold runaway electrons, produced by very strong electric fields, dominate the production of the X-rays.

Citation: Saleh, Z., J. Dwyer, J. Howard, M. Uman, M. Bakhtiari, D. Concha, M. Stapleton, D. Hill, C. Biagi, and H. Rassoul (2009), Properties of the X-ray emission from rocket-triggered lightning as measured by the Thunderstorm Energetic Radiation Array (TERA), *J. Geophys. Res.*, *114*, D17210, doi:10.1029/2008JD011618.

1. Introduction

[2] The search for X-ray emission from thunderstorms and lightning has a long history, beginning in the 1920s when C. T. R. Wilson first suggested that electrons could gain large energies from thunderstorm electric fields that exist in our atmosphere during electrically active times [*Wilson*, 1925]. These so-called runaway electrons occur when the force on the electrons, owing to an electric field, exceeds the effective frictional force, predominantly owing to ionization energy losses, that is experienced by the electrons as they move through air. Such runaway electrons can gain very large amounts of energy, reaching many tens of MeV in some cases [*Gurevich et al.*, 1992; *Gurevich and Zybin*, 2001]. As the runaway electrons collide with air they will emit bremsstrahlung X-rays, which can then travel several hundred meters at sea level, allowing runaway electrons and the conditions that created them to be studied remotely.

[3] Since the 1980s, evidence for X-ray emission from thunderstorms has been steadily building [*Dwyer et al.*, 2004a; *Tsuchiya et al.*, 2007]. For example, using aircraft observations made inside thunderstorms, *Parks et al.* [1981] and later *McCarthy and Parks* [1985] reported X-ray enhancements for several seconds in the time leading up to the lightning. Since the X-rays ceased when the lightning occurred, this emission has been interpreted as resulting from energetic electrons produced by the large-scale electric field inside the thunderstorm and not due to lightning. Later *Eack et al.* [1996, 2000] measured X-ray enhancements lasting up to 20 s from inside and above thunderstorms using balloon borne instruments. In 1994, intense terrestrial gamma ray flashes (TGFs) were reported using BATSE data

[1]Department of Physics and Space Sciences, Florida Institute of Technology, Melbourne, Florida, USA.
[2]Department of Electrical and Computer Engineering, University of Florida, Gainesville, Florida, USA.
[3]Roswell Park Cancer Institute, Buffalo, New York, USA.
[4]Department of Earth, Atmospheric and Planetary Sciences, Massachusetts Institute of Technology, Cambridge, Massachusetts, USA.

Copyright 2009 by the American Geophysical Union.
0148-0227/09/2008JD011618$09.00

from the Compton Gamma Ray Observatory (CGRO) [*Fishman et al.*, 1994]. These flashes were originally inferred to be associated with high-altitude discharges such as red sprites [*Nemiroff et al.*, 1997] largely because of their correlation with thunderstorms and lightning [*Inan et al.*, 1996]. However, recent measurements by the RHESSI spacecraft have shown that the thunderstorms are a more likely source for the TGF emission [*Smith et al.*, 2005; *Dwyer and Smith*, 2005; *Carlson et al.*, 2007].

[4] Until very recently, the evidence for X-ray emission from lightning has not been as strong. Many of the early results were either ambiguous or contradictory, in part owing to the unpredictability of lightning and the challenges of measuring energetic radiation in the electromagnetically noisy environment created by the lightning [e.g., *Schonland and Viljoen*, 1933; *Halliday*, 1934; *Hill*, 1963; *Shaw*, 1967; *D'Angelo*, 1987; *Suszcynsky et al.*, 1996; *Brunetti et al.*, 2000; *Chubenko et al.*, 2000; *Moore et al.*, 2001]. In hindsight, some of these earlier reports of energetic radiation from lightning were almost certainly correct. However, as recent as a few years ago, the general consensus was still that thunderstorms may produce X-ray emission but lightning probably did not. For example, Moore *et al.* reported the detection of energetic radiation during natural cloud-to-ground lightning [*Moore et al.*, 2001], but it was not clear whether the source of the energetic radiation was the lightning leader or the overhead thundercloud, similar to earlier measurements. Adding to the difficulty, the NaI detector used by Moore et al. could not determine whether the energetic radiation was made up of X-rays, gamma rays or energetic electrons; however, MeV gamma rays were suggested, making it impossible to estimate the distance to the source. Nevertheless, the results of Moore *et al.* renewed interest in the field and demonstrated that further study was warranted.

[5] The following year, *Dwyer et al.* [2003] discovered that rocket-triggered lightning also emits bright bursts of energetic radiation. Later, *Dwyer et al.* [2004b] showed that the detected energetic radiation was predominantly X-rays with energies usually extending up to about 250 keV and that the X-rays were emitted in discrete bursts lasting less than 1 μs in duration. These results showed that great care must be taken when interpreting energetic radiation pulses from lightning when using relatively slow detectors, such as NaI/PMT detectors, because of the X-rays pile up that causes large amounts of energy to be deposited in a very short time. *Dwyer et al.* [2004b] also showed that X-ray emissions originated from the last few hundred meters of the dart leader channel and that the source propagated downward with the leader as it approached the ground.

[6] Because the X-ray energies extend above 100 keV, thermal emission is virtually ruled out as being the source since the maximum temperature occurring during lightning, $\sim$30,000 K during the return stroke, is many orders of magnitude too low to account for such energetic X-ray emission. As a result, the only viable mechanism to explain this emission is through the production of runaway electrons in strong electric fields. However, exactly how and where these runaway electrons are generated remains under active debate. For instance, *Dwyer* [2004] demonstrated that the Relativistic Runaway Electron Avalanche (RREA) model [*Gurevich et al.*, 1992], which had been used for many years to model the TGF data could not explain the intensity and the X-ray spectra from lightning. *Dwyer* [2004] suggested that instead the runaway electrons were produced in the very strong electric fields near the leader tip or the streamer heads via the cold runaway electron mechanism [*Gurevich*, 1961; *Moss et al.*, 2006; *Dwyer*, 2008]. It is not known how large the electric field magnitudes can get during the dart-stepped leader propagation. For example *Lalande et al.* [2002] modeled the internal leader field and found that it peaked at about 500 kV/m. However, the work of *Moss et al.* [2006] suggests that the streamer heads produce fields over 3×10^7 V/m. If correct, it should be possible to use remotely measured characteristics of the X-ray emission to give information about the electric fields produced near the lightning, a measurement that is otherwise very difficult to make.

[7] In addition to the triggered lightning, *Dwyer et al.* [2005a] measured the X-ray emission from natural, negative cloud-to-ground lightning at the ICLRT. They showed that the X-ray emission from natural lightning was very similar to the emission from triggered lightning. They also demonstrated that the X-ray bursts were emitted during the step formation of the lightning stepped leader, identifying for the first time the production of the runaway electrons with a specific lightning process. *Howard et al.* [2008], using a time of arrival (TOA) technique, further showed that the X-ray bursts are emitted $\sim 0.1-1$ μs after the peak of the leader step dE/dt pulses and are located at approximately the same positions as the simultaneously observed dE/dt pulses, strengthening the connection between the X-ray emission and the stepping processes. The similarity between the dart leader emission from triggered lightning and the stepped leader emission from natural lightning is very interesting, considering that nearly every dart leader is observed to generate X-rays and yet not every dart leader is thought to involve stepping. The similarity in the X-ray emission suggests that all (negative) leader types involve stepping to some degree and, as a result, may bear more similarities than is apparent based upon optical and radio frequency measurements [*Dwyer et al.*, 2005a].

[8] Even though the early work of *Dwyer et al.* [2003, 2004b] uncovered some of the key features of the X-ray emission, this initial work used only a small number of instruments located near (within $\sim$50 m) the channel. Consequently, many of the properties were not determined. For example, only estimates of the X-ray luminosity of the dart leader channel were made and the angular distribution of the emission was not determined. The energy measurements made previously were also estimates and the inferred energy of the source energetic electrons were dependent upon assumptions of the geometry of the emission. In order to make improved measurements of natural and triggered lightning, the Thunderstorm Energetic Radiation Array (TERA) was constructed at the ICLRT starting in 2005 and began full-scale operation in 2007. In this paper, we report on the results of the X-ray emission from rocket-triggered lightning observed by TERA.

2. Instrumentation

[9] The Thunderstorm Energetic Radiation Array (TERA) is an experiment designed to measure energetic

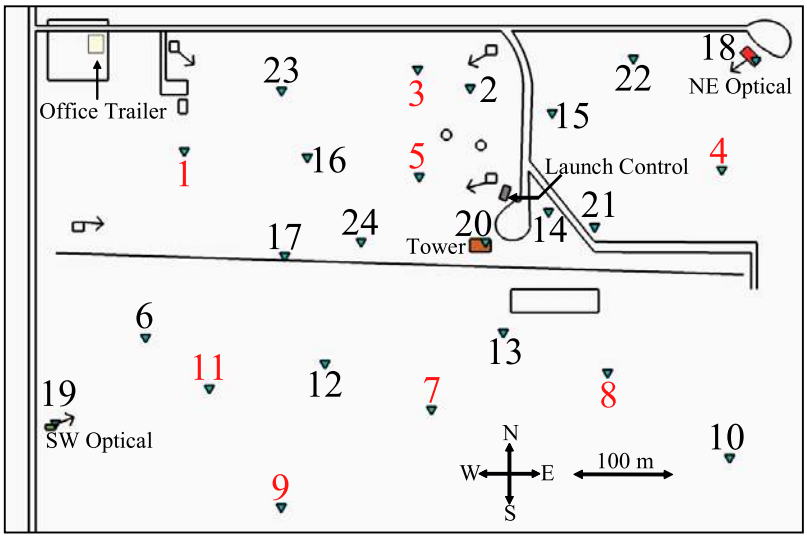

Figure 1. Overview of the ICLRT facility at Camp Blanding, Florida. Shown are the locations of the different stations centered on the rocket launch tower (marked in orange rectangle). Station 20 is located at the top of the launch tower 12 m above the ground. Stations allocated for the TOA network are marked in red.

radiation (X-rays and gamma rays) from thunderclouds and lightning. TERA is also part of an experiment called the Multiple Station Experiment (MSE), which is used to study the electric and magnetic fields from rocket triggered lightning and nearby natural lightning. Besides the X-ray detectors, the MSE/TERA stations are also equipped with instrumentation to measure electric fields and their derivatives as well as magnetic fields using flat plate antennas and loop antennas [*Jerauld*, 2007]. The flat plate antennas are used to measure the vertical component of the electric field and its derivative for nearby lightning. Owing to some charge movement during the leader formation process, a process which is still not yet fully understood, electromagnetic pulses are produced; these pulses are picked up by the sensitive antennas. After accounting for the propagation delay through the fiber optic and the electronics, the radiation source of these pulses is located using TOA techniques [*Howard et al.*, 2008] that are based on the arrival times of the *dE*/*dt* pulses. The 24 TERA instruments are distributed at different stations across the ~1 km^2 ICLRT site, centered around the rocket launch tower as shown in Figure 1.

[10] The 24 instruments that compose TERA are contained in 1/8″ (0.32 cm) thick aluminum boxes to shield the instrument from moisture and light [*Dwyer et al.*, 2003, 2004a, 2005b]. The aluminum box lids allowed X-rays with energies down to about 30 keV to enter from all directions, while acting as a Faraday cage to shield the instruments from external static electric fields and RF noise. The design of the TERA instruments is shown in Figure 2. Most of the instruments contain two 7.6 cm × 7.6 cm cylindrical NaI(Tl)/Photomultiplier tube (PMT) detectors as is shown in Figure 2. Five of the 24 instruments contain NaI(Tl)/PMT detector and one plastic scintillator (36 cm × 25 cm × 1 cm), the latter having a faster time response than the NaI scintillators. The NaI detectors were manufactured by Saint Gobain (3M3 series). The NaI scintillators were mounted to the PMTs and placed inside light-tight aluminum housings with

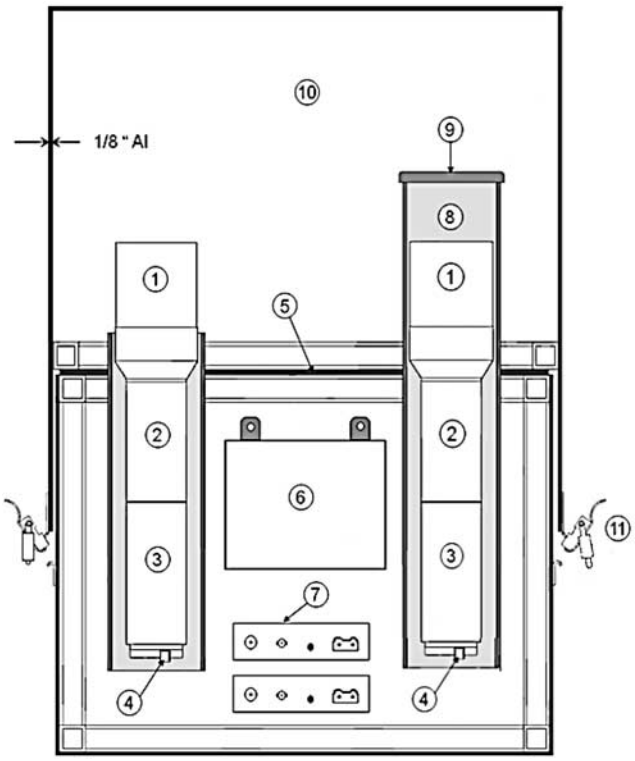

Figure 2. Schematic diagram of one of the X-ray instruments with attenuated and unattenuated detectors. The components are as follows: (1) 7.6- by 7.6-cm NaI scintillator; (2) photomultiplier tube (PMT) detector; (3) PMT base (HV supply and voltage divider); (4) PMT anode output, which connects directly to the fiber optic transmitter; (5) gasket; (6) 12-V battery; (7) FM fiber optic transmitters; (8) lead attenuator (also used as a collimator when the lead cap is removed); (9) lead cap; (10) 0.32-cm-thick aluminum box; (11) latches.

μ-metal shields. The NaI/PMTs were then mounted on Ortec photomultiplier tube bases (model 296), which contained internal HV supplies and divider chains. In addition, the NaI/PMT detectors, which are designed to be light-tight, were wrapped in black electrical tape on aluminum tape and were checked for light leaks with a bright strobe light before placing the detectors inside the 0.32 cm thick aluminum boxes. The plastic scintillator/PMT detector was manufactured by mounting a 5.08 cm diameter PMT to a light guide attached to the end of the scintillator. The assembly was then made light tight by wrapping it in black plastic. In this paper, only data from the NaI/PMT detectors will be reported.

[11] The aluminum boxes and their lids were both welded on eight seams. The lids slid over the bottom of the boxes like a shoe box with a 15 cm vertical overlap between the top and the bottom. The inside of the boxes were painted black to absorb any light that might enter through the gaskets. The instruments were powered by internal 12 V batteries. Opticomm FM (68 k-ohm input impedance, 30 MHz bandwidth) analog fiber optic links were used to transmit the signals from the PMT anodes directly to the data acquisition system located in a separate, shielded trailer. The armored fiber optic cables used each containing six channels (62.5 μm) and are laid across the field, providing the data and communication infrastructure for the whole site. All the fiber optic delays have been accurately measured from end to end in order to align the signal from different stations [*Howard et al.*, 2008].

[12] In each of the boxes with two NaI/PMT detectors, one detector is mounted inside a 0.32 cm thick lead tube that extends 4.5 cm above the top of the scintillators and covered with a lead cap of the same thickness. The lead also extends 41 cm below the scintillators, completely covering the PMTs and the bases. These lead attenuators absorb X-rays below 300 keV thereby helping determine the energy spectrum by comparing the signals from the unattenuated (with 30 keV cut-offs from the Al lids) and the attenuated detectors. In addition, two heavy aluminum boxes (XLBs) located at a distance of 10 m from the launch tower [*Dwyer*, 2004] are also used. These boxes contain a total of five detectors.

[13] The TERA instruments are powered on and off remotely using a set of PIC controllers that receive commands from the launch control via fiber optics. In addition to arming the system and switching on/off the instruments, these controllers monitor the temperatures and battery voltages and perform calibrations.

[14] The data acquisition system is triggered when the incident current measured from triggered lightning exceeds a threshold of 7 kA, or when two optical sensors, located at the northeast and southwest corners of the site, are simultaneously triggered owing to on-site natural lightning. Signals from all X-ray detectors and the MSE are recorded by Yokogawa 750 ScopeCorders, with 12 bit resolution and a sampling rate of 10 MHz. Exceptions are the XLBs, which are stored on a DL716 Yokogawa scope also operating at the same sampling rate.

[15] A subset of eight detectors from TERA, along with MSE instruments, called the time-of-arrival (TOA) network, are recorded using LeCroy Waverunner scopes that sampled at 250 MHz with 8 bit resolution, with a total record length of 2 and 1 μs of pretrigger sampling, allowing faster timing to help determine the location of the source of X-ray emissions and electric field changes. A description of the TOA network along with results is presented in the work of *Howard et al.* [2008].

[16] We note that no control (PMT without a scintillator) detector was used in the present experiments. Control detectors were previously used for the Marx generator experiments described by *Dwyer et al.* [2005a] and for most of the triggered lightning and natural lightning experiments at the ICLRT during the last 5 years. For all the X-ray observations of lightning and laboratory sparks, involving hundreds of measurements, no significant signal that might be confused with an X-ray measurement has ever been recorded on a control detector. Because the existence of X-ray emission from lightning and laboratory sparks is now well established, and because the performance of the instruments is well known, a control detector was no longer deemed necessary, so that channel was replaced with an active detector.

3. Observations

[17] Over the course of its operation, from 2005 until it became fully operational in 2007, TERA-MSE has recorded seven successful rocket triggered lightning flashes, with a total of 13 return strokes. It has also recorded 18 natural flashes, all negative cloud-to-ground. Almost all of the observed discharges have produced energetic radiation in the TERA detector records [*Dwyer et al.*, 2005a; *Howard et al.*, 2008]. For internal bookkeeping, we tagged our recorded files as MSE and UF for natural and triggered events, respectively, followed by the year and the flash number, and each event is tagged with a GPS time stamp.

[18] This study has four main objectives: (1) obtaining an empirical relation for the radial distribution of X-ray emission, (2) estimating the energy spectrum of the X-rays and the energetic electrons that produce the X-rays; (3) inferring the luminosity evolution of the energetic electrons and X-ray source as it propagates, and (4) examining the angular distribution of the energetic electrons producing the observed X-ray emissions. We would like to mention that the term luminosity refers to the production rate (number/s) of energetic electrons and X-rays. For these objectives, we will focus on three rocket triggered lightning events (UF-0501 and UF-0503 on 2 July 2005, and UF-0707 on 31 July 2007). The X-ray intensities for these events were large enough that they were easily registered by our distant detectors at the edges of the ICLRT. Both the UF-0501 and UF-0503 events were triggered from a mobile launcher at the edge of ICLRT site (close to station 4 in Figure 1). As a result, we have measurements out to a radial distance of 500 m, greater than for triggers from the launch tower at the center of the site. The UF-0707 event was triggered from the launch tower, close to the center of TERA (station 20 in Figure 1). This event, which was identified as a dart-stepped leader [*Howard et al.*, 2008] compared to the other two events which are normal dart leaders, is the most intense of the three and lasted for about 200 μs (as compared to 30 μs for the other two events), so it provides the best picture of the X-ray source evolution.

[19] Figure 3 shows the waveforms of the electric current measured at the launch tower along with the electric field at

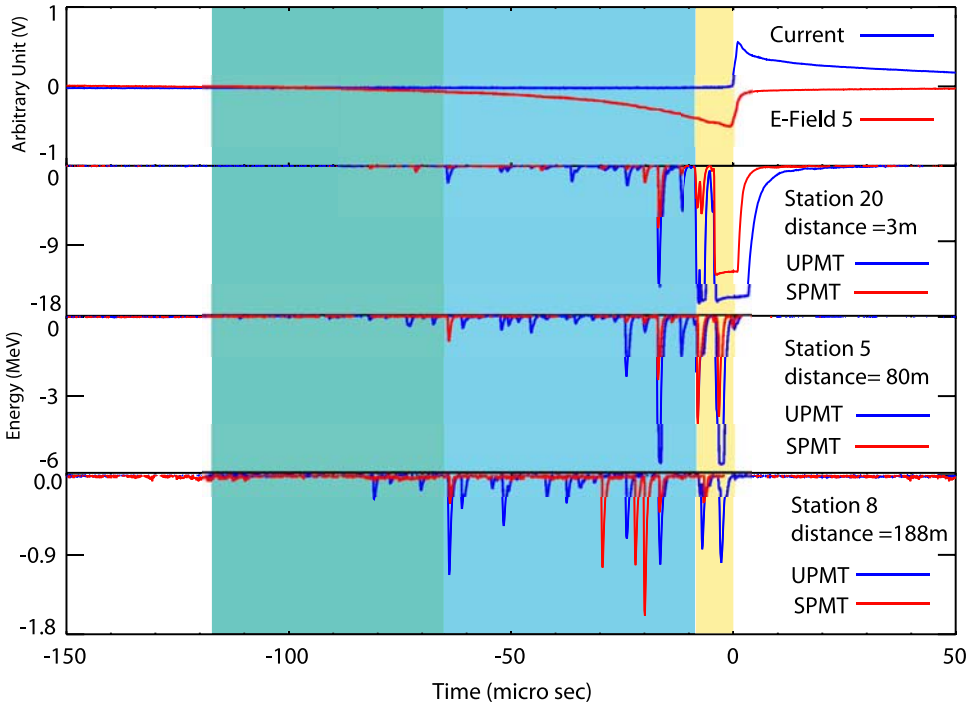

Figure 3. Waveforms of the electric current measured at the launch tower along with the electric field at station 5. Also shown are the waveforms from different X-ray detectors located at 3, 80, and 188 m from the lightning channel, arranged from top to bottom. Both shielded and unshielded detectors at each station are shown on the same plot. Color-highlighted time zones correspond to the source at different altitudes used in the analysis.

station 5. It also shows a sample of the X-ray waveforms from six detectors, three shielded (i.e., attenuated) with lead (SPMT) and three unshielded (i.e., unattenuated) (UPMT), for the UF-0707 event. These observations are from three stations, located at 3, 80, and 188 m from the launch tower (stations 20, 5, and 8 in Figure 1). Each plot shows the signal from the PMT anodes as a function of time. Each negative pulse seen in the plots corresponds to a burst of X-rays detected by the NaI/PMTs, and the amplitude of each signal is a direct measure of the X-ray energy deposited in the NaI. The return stroke occurs at time $t = 0$, so the X-rays are being measured during the dart leader phase, that is as the dart leader (in this case dart-stepped leader) propagates from the cloud to the ground.

[20] As can be seen, the observed X-ray intensity from triggered lightning generally decreases as we move away from the lightning channel. In addition, the observed intensity generally increases as the X-ray source approaches the ground, reaching a peak intensity immediately prior to the return stroke (time zero) where the X-ray source is presumably closest to the ground. The emission ceases after the start of the return stroke. We note that the lightning channel terminates at the top of the rocket launcher which is located approximately 17 m above the ground level. As a result, the time of the return stroke corresponds to the time where the dart leader attaches to the top of the launch tower and not the ground. Owing to the relatively slow response time of NaI/PMT detectors, the X-rays arriving over a very short period of time can pile up causing nearby detectors to saturate. This saturation, which is clearly seen as a clipping of the pulses in the top plot, is due primarily to the fiber optic transmitter receivers, which limit the voltage to ±1 V.

[21] On closer inspection, data shown in Figure 3 reveals that despite often having deposited energies of many MeV, these X-ray pulses are usually not individual gamma ray photons. Instead the X-rays arrive in discrete bursts lasting less than 1 μs in duration. Because the 0.3 mm thick lead attenuators are transparent to gamma rays above about 300 keV, if the pulses seen in Figure 3 were individual gamma rays then there should not be large differences in the signals seen from the detectors with and without the lead shielding. A comparison of the signals from the attenuated and unattenuated detectors in the same boxes confirm that the large pulses are not individual gamma rays, but instead are composed of bursts of lower-energy X-rays. The response of the attenuated detectors will be discussed further in section 5.

[22] In order to extract the deposited energy from the data, we fit the instrument response to the data as shown in Figure 4. For comparison, the top inset shows a close-up of a pulse produced by the detection of a single Cs-137 662 keV gamma ray made by temporarily placing a radioactive source on top of one of the instruments. Also shown in the inset is the fit of the detector response function, which is determined by the front end electronics and the NaI light decay time. The response function fits both the Cs-137 gamma ray data and natural background data (cosmic rays and ambient X-rays) as well.

[23] After the amplitudes of these X-ray bursts are found by fitting the response function, the deposited energy is determined by multiplying the signal amplitudes by a

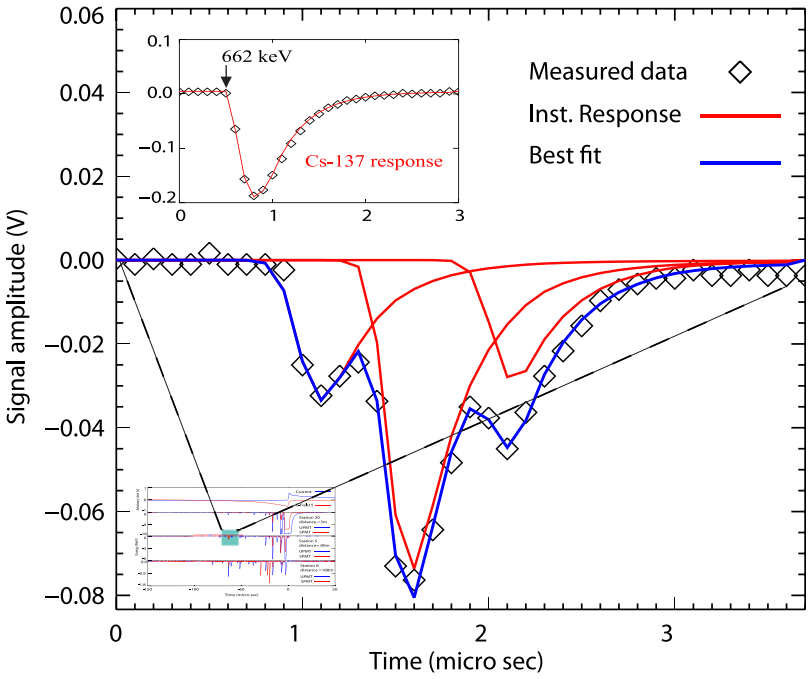

Figure 4. An expanded view of the X-ray waveform from one of the detectors over a few microsecond period. Diamonds indicate the measured X-ray data and the red traces indicate the individual instrument responses corresponding to photons with different energies. The overall fit shown in blue closely match the measured data. The top inset shows the response of one of the NaI/PMT detectors for a single 662 keV gamma ray from a CS-137 radioactive source. The solid red line represents the instrument response derived from the electronics, and the NaI decay time units on both time axis are in microseconds.

calibration factor for each detector. The energies measured by the detectors are calibrated with a Cs-137 radioactive source, placed temporarily on each box.

[24] Figure 5 shows the measured total deposited energies for all unshielded (UPMT) detectors for the three triggered flashes as a function of radial distance from the lightning channel. The base of the arrows indicates the lower limit on the energy deposited for the saturated detectors near the lightning channel. For this radial energy distribution study, we averaged the data from equidistance detectors from the channel. As can be seen, all three flashes have a similar radial dependence of the deposited energy. Furthermore, the deposited energy fits the empirical expression $\propto[\exp(-r/120)]/r$. As will be shown later, this radial fall off arises from a combination of the $1/r$ decrease from a source along a line path and the X-ray absorption and scattering with air and the ground, due predominately to photoelectric absorption and Compton scattering.

[25] Because the entire data records are 2.2 s long with a 1-s pretrigger sampling, we are able to determine the rate of background energy deposited on the detectors prior to and after the time of the return strokes. The average background rate was found to be 80 and 60 MeV/s on each unshielded and shielded detectors, respectively. As a result, for the 200-μs-long event presented here, at most only 16 keV is expected owing to background.

4. Modeling

[26] Here we use detailed Monte Carlo simulations to investigate properties of the energetic electron source populations that produce these X-rays. As with many energetic particle instruments, Monte Carlo simulations are a useful tool for understanding the response of the TERA instrument. Because the array elements are distributed over many hundreds of meters on the ground, the effect of the X-ray propagation through the air and interaction of the X-rays with the ground must be considered.

[27] For this work, a detailed 3-D Monte Carlo simulation [*Dwyer*, 2003, 2004, 2007; *Coleman and Dwyer*, 2006] has

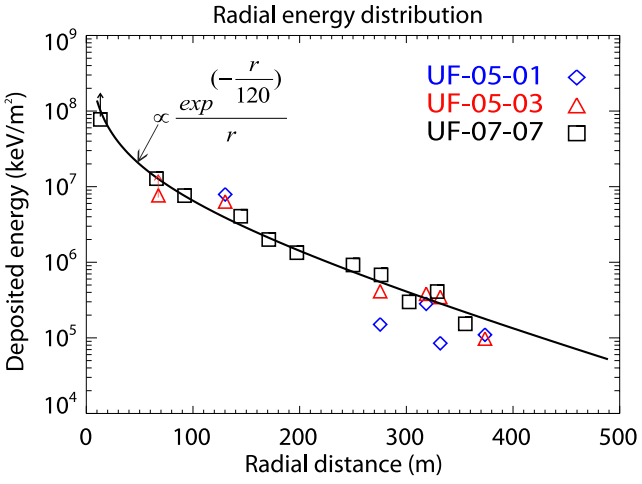

Figure 5. Energy deposited on the unshielded detectors versus their radial distance from the lightning channel for the three rocket triggered events. The radial falloff is proportional to $\propto[\exp(-r/120)]/r$ as shown with solid line. The base of the arrows indicates the lower limit on the energy deposited for the saturated detectors.

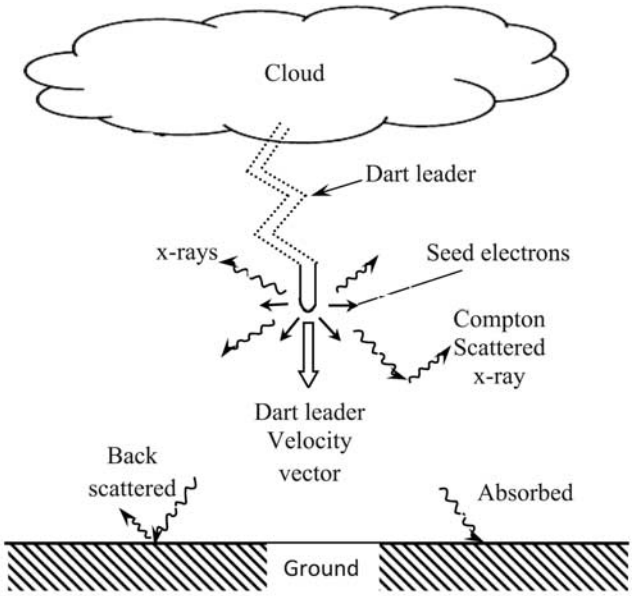

Figure 6. Schematic diagram showing the model used to simulate X-ray emission from lightning. It shows the dart leader initiated inside the cloud and propagating downward to the ground; it also shows the electrons (straight arrows) being emitted near the leader tip isotropically which in turn produces X-rays (squiggly arrows).

been used to model the bremsstrahlung emission of energetic electrons and the propagation of the X-rays through air, including interactions with the ground and the detectors. This simulation includes, in an accurate form, all the important interactions involving energetic electrons, positrons, X-rays and gamma rays. These interactions include energy losses through ionization and atomic excitation, and Moller scattering. The simulation fully models elastic scattering using a shielded-Coulomb potential and includes bremsstrahlung production of X-rays and gamma rays, and the subsequent propagation of the photons, including photoelectric absorption, Rayleigh scattering, Compton scattering, and pair production. The simulation also includes absorption and backscatter of X-rays from the soil and interactions of the X-rays with the aluminum, lead and NaI in the instruments.

[28] The strong correlation between X-ray emission and the stepping process in natural lightning stepped leaders [*Dwyer et al.*, 2005a; *Howard et al.*, 2008] suggests that the source, i.e., the energetic runaway electrons, must have been generated locally owing to high electric fields near the natural lightning leader steps. As a result, in this model, it is assumed that most of the acceleration of the energetic electrons that produce the X-rays occurs over a very short distance in the high field region near the dart leader. These electrons are injected into the simulation with an exponential energy spectrum with the *e*-folding kinetic energy, K_o, left as a free parameter: $dN_e/dK \propto \exp(-K/K_o)$. This spectral form is motivated by the fact that in the regime where relativistic runaway electron avalanche (RREA) multiplication occurs, the energy spectrum is approximately exponential with an *e*-folding energy of 7.3 MeV [*Lehtinen et al.*, 1999; *Dwyer*, 2004]. For simplicity, it is assumed that the effect of the ambient electric field is negligible compared to the enhanced fields around the leader tip and so the electric field is set to zero throughout the simulation.

[29] The simulations are done on the basis of the model pictured in Figure 6. After the initial stages of rocket triggered lightning, following the vaporization of the trailing wire and the initial continuous current (ICC) [*Olsen et al.*, 2006], a dart leader is initiated inside the cloud and propagates downward almost following the path left behind by the vaporized wire. In this case the leader is a dart-stepped leader, since it moves in discrete steps accompanied by electromagnetic pulses and followed by X-ray emission which are spatially colocated [*Howard et al.*, 2008]. The dart-stepped leader is depicted as a vertical channel as shown in Figure 6. Using the approximate locations of X-ray and *dE*/*dt* pulses from the TOA [*Howard et al.*, 2008], we can estimate the location and velocity of the source. J. Howard et al. (RF and X-ray source locations during the lightning attachment process, submitted to *Journal of Geophysical Research*, 2009) shows that the leader (i.e., UF-0707) propagated from 330 m down to 75 m at an constant speed of 4.8×10^6 m/s, which is used throughout the analysis. For each time we then calculate a source altitude based upon this data. Because the X-ray data is binned into time, the simulation also uses the same time periods with the source assumed to be emitting X-rays at constant luminosity during that period with the position and velocity estimated from the TOA data. The energetic electrons are injected into the Monte Carlo simulation at those heights and propagated until they stop, and the bremsstrahlung X-ray emission from the energetic electrons is calculated. The Monte Carlo simulation then propagates the photons until they are absorbed or fall below a minimum energy threshold (30 keV). The simulation keeps track of all the X-rays that hit the ground (detector plane). The ground plane is divided into different zones (annuli) and all X-rays that fall within each annulus are recorded. The Monte Carlo also calculates the instrument response, including the effects of the aluminum lids, the lead attenuators and the NaI scintillators, and determines the expected deposited energy in the NaI for each detector. Many simulations are run with different angular distributions of the electrons and with different electron energy spectra and these results (deposited energies) are compared to the data.

5. Results

[30] Many exponential energy distributions (for clarity only three are shown in Figures 7 and 8) for the energetic electrons have been modeled to cover the energy range of interest, from a few hundred keV extending up to 7 MeV. The data used for this analysis are for the rocket-triggered event UF-0707. Note that the 7 MeV spectrum is what is expected if significant relativistic runaway electron avalanche (RREA) multiplication are occurring [*Dwyer*, 2004]. In Figure 7, the source is modeled as a narrow beam directed downward. In other words, the energetic electrons are injected straight down. However, after injection and owing to elastic scattering with air atoms, the energetic electrons experience angular diffusion causing the angular distribution to become more isotropic as they lose energy. In addition, the bremsstrahlung emission also has a broad

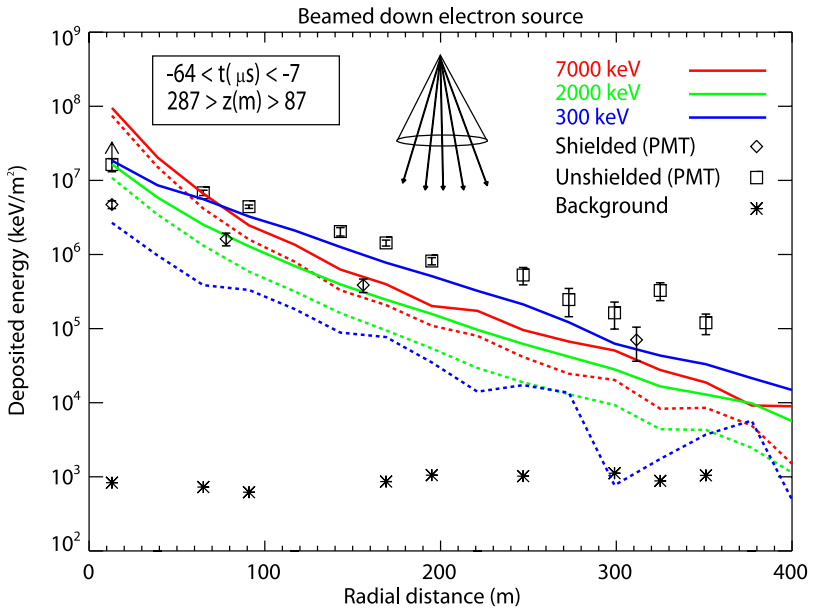

Figure 7. Monte Carlo simulation results for three different electron energy distributions for a downward beamed energetic electron source. Solid lines (model) and square data points are the energy deposited on the unshielded detectors, while the dashed lines (model) and diamond signs are the shielded detectors. The asterisk shows the estimated background energies for the same time period of 57 μs.

angular distribution at these energies ($\theta \sim 1/\gamma$ where γ is the Lorentz factor of the electrons). Both of these effects are fully modeled by the Monte Carlo. Figure 7 shows the observed X-ray deposited energies along with the model results. In Figure 7 both the unattenuated and attenuated detectors are shown along with the estimated background. In Figures 7 and 8, only X-ray data between 7 and 64 μs before the return stroke are used, corresponding to the dart-stepped leader in the middle altitude range for these observations of 287 m down to 87 m above the ground. To calculate the error bars in all the plots, the Monte Carlo simulations were used to estimate the RMS fluctuations in the deposited energies that should occur. In other words, the simulation predicts the deposited X-ray energies, which were fit to the observed data, along with the fluctuations in these energies that would be observed if the experiments

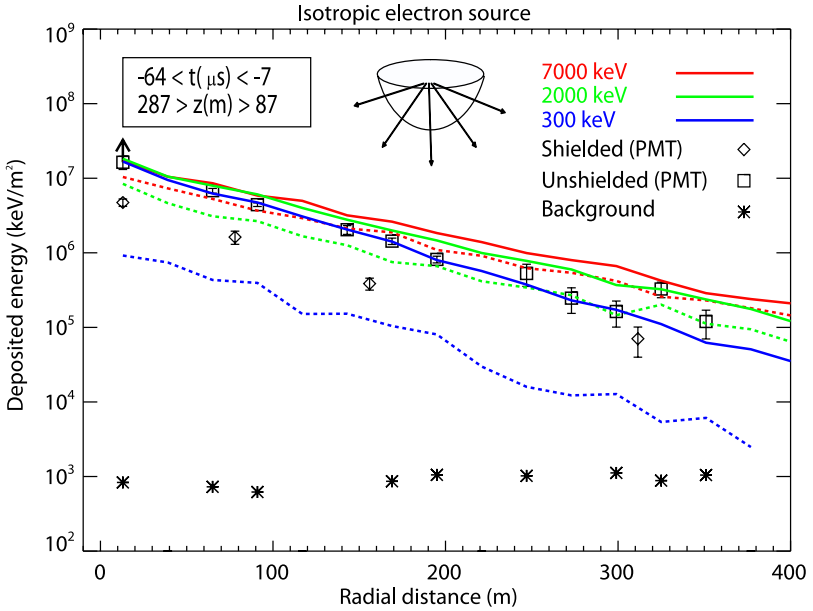

Figure 8. Monte Carlo simulation results for three different electron energy distributions for an isotropic energetic electron source. Solid lines (model) and square data points are the energy deposited on the unshielded detectors, while the dashed lines (model) and diamond signs are the shielded detectors. The asterisk shows the estimated background energies for the same time period of 57 μs.

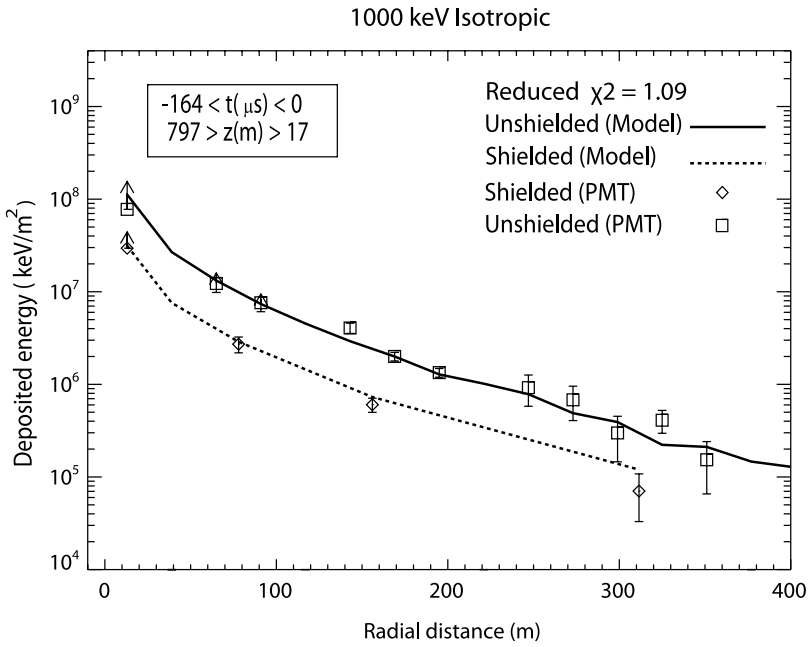

Figure 9. Monte Carlo simulation results for a 1-MeV (*e*-folding energy) isotropic energetic electron source for all altitudes and overall time period. Solid lines (model) and square data points are the energy deposited on the unshielded detectors, while the dashed lines (model) and diamond signs are the shielded detectors.

were repeated many times. This method is necessary since the number of photons detected and hence the Poisson fluctuations are not known a priori, and modeling is needed to estimate the photons' energy. As can be seen, all three simulations significantly underestimate the deposited energy at larger radial distances and produced a fit with reduced χ^2 of 6.6, 5.1, and 10.4 for the electron energy distributions of 7, 2, and 300 keV, respectively.

[31] Alternatively, instead of a beamed electron source, if we inject the energetic electrons with an initial isotropic distribution into the lower hemisphere, we get the model results shown in Figure 8. Note that the isotropic distribution is a noticeably better fit than the beamed distribution with reduced χ^2 of 2.6, 1.5, and 5.6 for the electron energy distributions of 7, 2, and 300 keV, respectively. It is found that an isotropic electron source with an average energy of 1 MeV is the best fit case with reduced χ^2 of 1.09 as shown in Figure 9. The background level shown in Figures 7 and 8 is insignificant compared to the measured energies and will not be included in further plots.

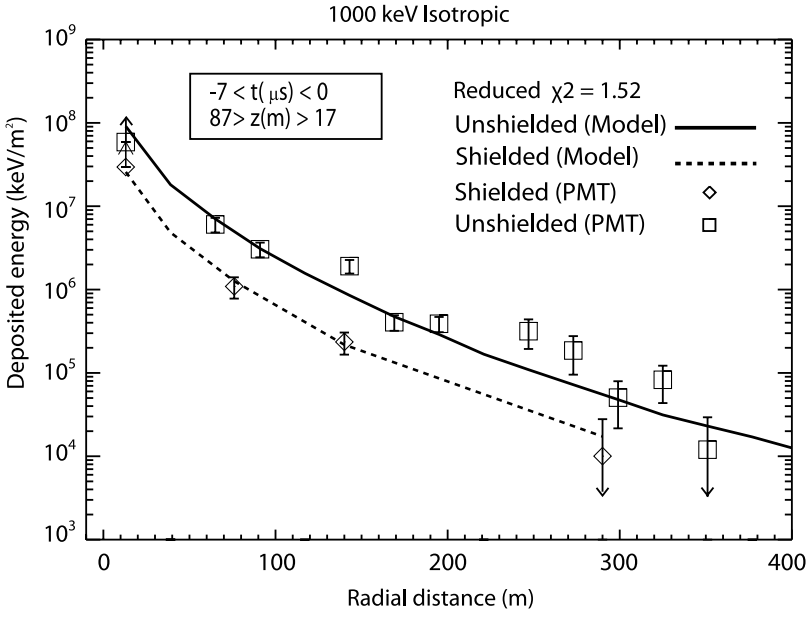

Figure 10. Same as Figure 9 except that the source altitude range is limited to 17 and 87 m.

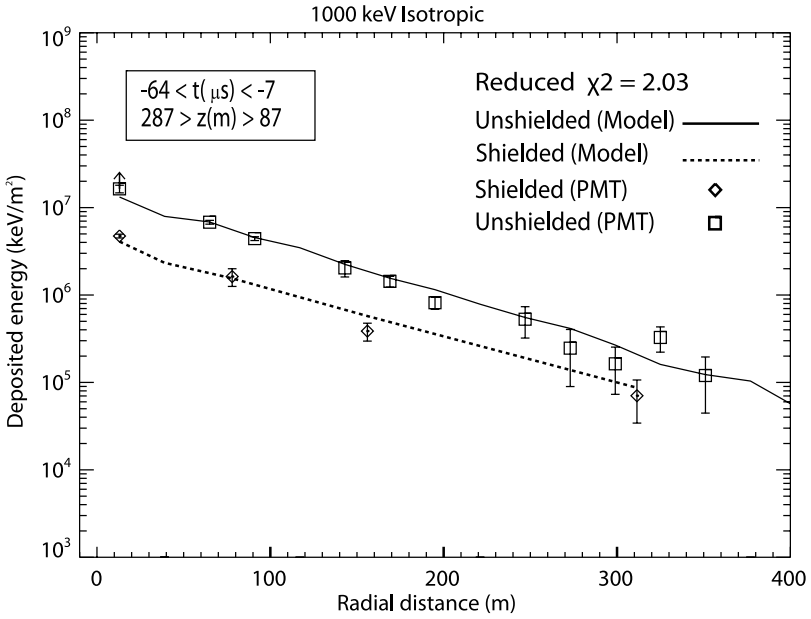

Figure 11. Same as Figure 9 except that the source altitude range is limited to 87 and 287 m.

[32] In Figure 9, we considered the total energy deposited over all time periods from -164 μs to the time of the return stroke (t = 0). Using the average speed of the dart-stepped leader of 4.8×10^6 m/s (J. Howard et al., submitted manuscript, 2009) we estimated the height of the source (i.e., the dart-stepped leader) between 17 m and 797 m. Figure 9 shows the consistency of the model with the measurement. In this plot and the ones that follow in Figures 10–12 , the overall normalization factor is a free parameter that is chosen to fit the data using least square fit method and then used to determine the production rate (luminosity) of the energetic electrons. It is found that the average rate of production of energetic electrons at the source is 1.3×10^{16} electron/s.

[33] We can now use this model and compare the results to subsets of the data corresponding to different source altitude ranges. Starting from the bottom of the channel, data for the last 70 m where the attachment process takes place as shown in Figure 10, is in good agreement with 1 MeV isotropic source model. However, owing to saturation on the detectors near the channel, we cannot rule out that very near the ground, the electrons are more downward than at higher altitudes. As we go to higher altitudes between 87 m and 287 above the ground, which is -7 to -64 μs prior to the return stroke as shown in Figure 11, the radial energy distribution starts to gradually decrease when the source is further from the detectors.

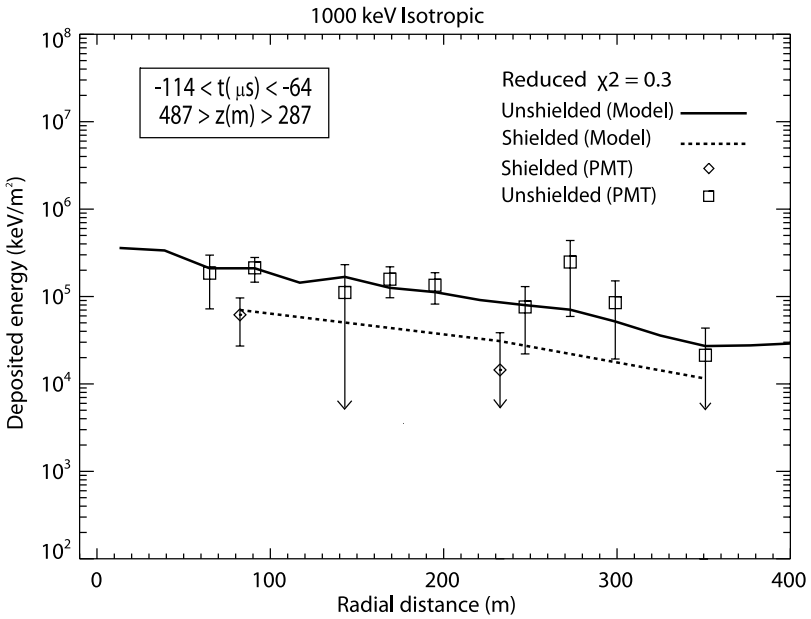

Figure 12. Same as Figure 9 except that the source altitude range is limited to 287 and 487 m.

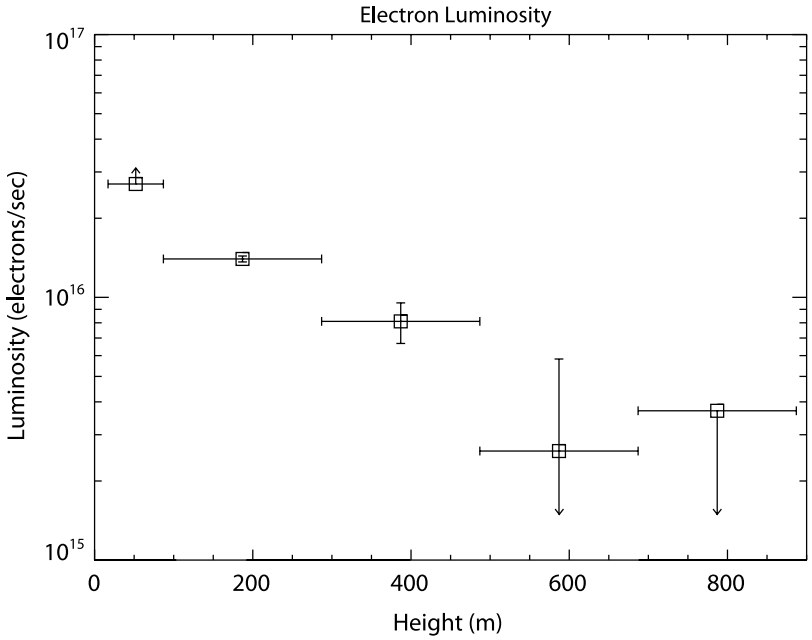

Figure 13. The luminosity of energetic electrons emitted by the dart-stepped leader versus altitude. The tails of the arrows set a lower and upper limit on the luminosity of the source owing to the saturation of detectors at the lower attitude and for no measurement on the ground at higher altitudes.

[34] Since the exact locations of the leader steps (dE/dt) are not known for altitudes above 330 m (J. Howard et al., submitted manuscript, 2009), it is assumed that the dart-stepped leader traveled downward along the same vertical path with the same velocity as below 330 m. Figure 10 shows the fit of the 1 MeV isotropic model described above to the subset of the data from -114 to -64 μs before the return stroke, which corresponds to an altitude range of 487 m down to 287 m. As can be seen, at higher altitudes, because the electron source is more equidistant from all the detectors, they tend to be illuminated by X-rays more uniformly. As we go earlier in time, from -164 to -114 μs prior to the return stroke, few X-rays were detected. As will be shown in Figure 13, the reduction in the intensity of X-rays detected compared to lower altitudes cannot be explained just by the increased distance to the detectors. In addition, the luminosity of the electrons and the emitted X-rays must also be reduced.

[35] At higher altitudes above 647 m, no emission was measured by the detectors. Assuming the same emission model used at lower altitudes still applies above 647 m, Monte Carlo simulations show that the luminosity cannot be greater than 3.7×10^{15} electron/s in order to be consistent with no X-rays being detected on the ground.

[36] The luminosity of energetic electrons above 30 keV versus altitude is determined from the fits shown in Figures 10–12. This is presented in Figure 13, which shows the average electron luminosity calculated in each altitude range versus source (dart-stepped leader) altitude. As can be seen there is a systematic decrease in the energetic electron luminosity with increasing altitude above the ground. Very near the ground, the average luminosity for this triggered lightning event reached about 2.7×10^{16} electron/s for the electrons. The conversion factor between energetic electrons and X-rays above 30 keV at the source is 0.13, which results in maximum X-ray luminosity of 3.5×10^{15}/s. We have also estimated the total X-ray energy deposit at the ground for this event is 10^{12} MeV.

6. Discussion

[37] Matching the output of the Monte Carlo simulation with the energy deposited on both the shielded and unshielded detectors, we can deduce that the source is most consistent with an isotropic electron emission with a characteristic energy of $\sim$1 MeV. The following scenario is most consistent with the data. The X-ray source propagates downward along the same path and with the same speed as the dart-stepped leader. The X-ray emission is consistent with bremsstrahlung emission from energetic electron interactions with air with the energetic electrons injected with the spectrum $dN_e/dK \propto \exp(-K/1\ \mathrm{MeV})$ and subsequently lose their energy in the air. Note that the exact shape of the energy spectrum was not determined, only the characteristic energy. Furthermore, the X-ray observations are not consistent with the source electrons initially beamed downward toward the ground, but rather are most consistent with the electrons emitted isotropically from the dart-stepped leader source. Note that the source was assumed to be isotropic in the lower hemisphere, however modeling a fully isotropic source did not affect the results but might lead to a higher luminosity. Owing to saturation on near by detectors, we cannot rule out the possibility that the source becomes slightly beamed when the leader is very close to the ground or a different source of emission is involved during the return stroke phase. The luminosity of the energetic electrons and hence the emitted X-rays decreased with increasing altitude up to 647 m. At higher altitudes above 647 m, no emission was measured by the detectors. The cause of the altitude variation in the luminosity is not known, but one

plausible explanation is the image charge of the dart leader as it approaches the ground increases the electric field allowing more energetic electrons to be produced.

[38] The energy spectrum of the energetic electrons, with 1 MeV characteristic energy, extends to higher energies than the 250 keV maximum energy reported by *Dwyer* [2004]. The difference could be due in part to the fact that *Dwyer* [2004] assumed that the X-rays were beamed downward, rather than isotropically emitted as has been found here. Since the isotropic emission will result in relatively more Compton scattered X-rays being detected, this can lower the estimated energy of the source electrons. In addition, the event UF-0707 studied in this paper is a dart-stepped leader with a peak current of 44 kA, which is relatively high compared to other triggered events with smaller peak currents of 10–15 kA [*Rakov and Uman*, 2003], and so this event could be producing a spectrum that extends to higher energies than those reported by *Dwyer* [2004]. Since no detailed analysis was performed for events UF-0501 and UF-0503, their characteristic energy was not determined. More important, however, a point of agreement between these result and those of *Dwyer* [2004] is that the energy spectrum from triggered lightning is too soft to be consistent with relativistic runaway electron avalanche (RREA) models, since in such models the average energy of the runway electrons is 7.3 MeV. Because runaway electrons produced by electric fields in air is at present the only viable mechanism for explaining the X-ray emission from lightning, the fact that the RREA model does not explain the emission suggests that instead so-called cold runaway (also known as thermal runaway) breakdown is responsible for the runaway electron production [*Dwyer*, 2004; *Moss et al.*, 2006]. In cold runaway breakdown, very strong electric fields, >30 MV/m cause the high-energy tail of the bulk free electron population to grow, allowing some electrons to runaway to high energies. Such very high fields may be present at streamer heads or leader tips or possibly in the lower-density leader channel [*D'Angelo*, 1987]. If this is the case, then the electric fields produced by leader and/or streamers is much larger than might be expected. Indeed, once the physics of the runaway electron production is better understood it may be possible to use the X-ray measurements as a probe of electric field conditions in lightning.

[39] The luminosity of the runaway electrons has implications for terrestrial gamma ray flashes (TGFs). On the basis of RHESSI observations and modeling, it is now thought that most TGFs originate from 15 to 21 km altitudes, possibly from within thunderclouds. *Dwyer and Smith* [2005] estimated that for a TGF source altitude of 15 km, 10^{17} relativistic runaway electrons must be present at the source in order to account for the flux of gamma rays seen from space by RHESSI. Based upon previous triggered lightning measurements, *Dwyer* [2007] estimated that this number of runaway electrons could be explained by lightning leader emissions assuming that additional avalanche multiplication on the order of 10^5 was occurring. If we take the luminosity of 2.7×10^{16} electron/s found in this work, and use a typical TGF duration of 1 μs, this results in 2.7×10^{13} energetic seed electrons per TGF per leader. If one such leader was propagating in a high field region within the thundercloud with the RREA multiplication factor of 10^5, then the flux of TGF could be explained. As an example, a multiplication factor of 10^5 can be obtained if the electric field is 400 kV/m (n/n_o), where n and n_o are the densities of air at the source altitude and at sea level, respectively, and the potential difference in the high field region is 270 MV. Because a leader propagating through an external high field region might be expected to generate at least as many energetic electrons as near the ground and high field regions above the runaway electron avalanche threshold are not uncommon inside thunderclouds, it is reasonable that TGF-like events with very large fluxes of energetic electrons and X-rays/gamma rays may be quite common inside thunderclouds.

[40] **Acknowledgments.** The authors would like to thank Maher A. Dayeh at Southwest Research Institute for the helpful discussions on this manuscript. The work was supported in part by NSF grants ATM 0420820, ATM 01337773, ATM 0607885, as well as DARPA grant HR0011-08-1-0088.

References

Brunetti, M., S. Cecchini, M. Galli, G. Giovannini, and A. Pagliarin (2000), Gamma ray bursts of atmospheric origin in the MeV energy range, *Geophys. Res. Lett.*, *27*, 1599–1602, doi:10.1029/2000GL003750.

Carlson, B. E., N. G. Lehtinen, and U. S. Inan (2007), Constraints on terrestrial gamma ray flash production from satellite observation, *Geophys. Res. Lett.*, *34*, L08809, doi:10.1029/2006GL029229.

Chubenko, A. P., V. P. Antonova, S. Y. Kryukov, V. V. Piskal, M. O. Ptitsyn, A. L. Shepetov, L. I. Vildanova, K. P. Zybin, and A. V. Gurevich (2000), Intense X-ray emission bursts during thunderstorms, *Phys. Lett. A*, *275*, 90–100, doi:10.1016/S0375-9601(00)00502-8.

Coleman, L. M., and J. R. Dwyer (2006), The propagation speed of runaway electron avalanches, *Geophys. Res. Lett.*, *33*, L11810, doi:10.1029/2006GL025863.

D'Angelo, N. (1987), On X rays from thunderclouds, *Ann. Geophys.*, *5B*, 119–122.

Dwyer, J. R. (2003), A fundamental limit on electric fields in air, *Geophys. Res. Lett.*, *30*(20), 2055, doi:10.1029/2003GL017781.

Dwyer, J. R. (2004), Implications of X-ray emission from lightning, *Geophys. Res. Lett.*, *31*, L12102, doi:10.1029/2004GL019795.

Dwyer, J. R. (2005), The initiation of lightning by runaway air breakdown, *Geophys. Res. Lett.*, *32*, L20808, doi:10.1029/2005GL023975.

Dwyer, J. R. (2007), Relativistic breakdown in planetary atmospheres, *Phys. Plasmas*, *14*(4), 042901, doi:10.1063/1.2709652.

Dwyer, J. R. (2008), Source mechanisms of terrestrial gamma ray flashes, *J. Geophys. Res.*, *113*, D10103, doi:10.1029/2007JD009248.

Dwyer, J. R., and D. M. Smith (2005), A comparison between Monte Carlo simulations of runaway breakdown and terrestrial gamma ray flash observations, *Geophys. Res. Lett.*, *32*, L22804, doi:10.1029/2005GL023848.

Dwyer, J. R., et al. (2003), Energetic radiation produced during rocket-triggered lightning, *Science*, *299*, 694, doi:10.1126/science.1078940.

Dwyer, J. R., et al. (2004a), A ground level gamma ray burst observed in association with rocket-triggered lightning, *Geophys. Res. Lett.*, *31*, L05119, doi:10.1029/2003GL018771.

Dwyer, J. R., et al. (2004b), Measurements of X-ray emission from rocket-triggered lightning, *Geophys. Res. Lett.*, *31*, L05118, doi:10.1029/2003GL018770.

Dwyer, J. R., et al. (2005a), X-ray bursts associated with leader steps in cloud-to-ground lightning, *Geophys. Res. Lett.*, *32*, L01803, doi:10.1029/2004GL021782.

Dwyer, J. R., H. K. Rassoul, Z. Saleh, M. A. Uman, J. Jerauld, and J. A. Plumer (2005b), X-ray bursts produced by laboratory sparks in air, *Geophys. Res. Lett.*, *32*, L20809, doi:10.1029/2005GL024027.

Eack, K. B., W. H. Beasley, W. D. Rust, T. C. Marshall, and M. Stolzenburg (1996), X-ray pulses observed above a mesoscale convection system, *Geophys. Res. Lett.*, *23*, 2915–2918, doi:10.1029/96GL02570.

Eack, K. B., D. M. Suszcynsky, W. H. Beasley, R. Roussel-Dupre, and E. Symbalisty (2000), Gamma ray emission observed in a thunderstorm anvil, *Geophys. Res. Lett.*, *27*, 185–188, doi:10.1029/1999GL010849.

Fishman, G. J., et al. (1994), Discovery of intense gamma-ray flashes of atmospheric origin, *Science*, *264*, 1313–1316, doi:10.1126/science.264.5163.1313.

Gurevich, A. V. (1961), On the theory of runaway electrons, *Sov. Phys. JETP, Engl. Transl.*, *12*(5), 904–912.

Gurevich, A. V., and K. P. Zybin (2001), Runaway breakdown and electric discharges in thunderstorms, *Phys. Uspekhi*, *44*, 1119–1140, doi:10.1070/PU2001v044n11ABEH000939.

Gurevich, A. V., G. M. Milikh, and R. A. Roussel-Dupré (1992), Runaway electron mechanism of air breakdown and preconditioning during a thunderstorm, *Phys. Lett. A*, *165*, 463–468, doi:10.1016/0375-9601(92)90348-P.

Halliday, E. C. (1934), Thunderstorms and the penetrating radiation, *Proc. Cambridge Philos. Soc.*, *30*, 206–215, doi:10.1017/S0305004100016649.

Hill, R. D. (1963), Investigation of electron runaway in lightning, *J. Geophys. Res.*, *68*, 6261–6266.

Howard, J., M. A. Uman, J. R. Dwyer, D. Hill, C. Biagi, Z. Saleh, J. Jerauld, and H. K. Rassoul (2008), Co-location of lightning leader X-ray and electric field change sources, *Geophys. Res. Lett.*, *35*, L13817, doi:10.1029/2008GL034134.

Inan, S. U., S. C. Reising, G. J. Fishman, and J. M. Horack (1996), On the association of terrestrial gamma ray bursts with lightning and implications for sprites, *Geophys. Res. Lett.*, *23*, 1017–1020, doi:10.1029/96GL00746.

Jerauld, J. (2007), Properties of natural cloud-to-ground lightning inferred from multiple-station measurements of close electric and magnetic fields and field derivatives, Ph.D. thesis, Univ. of Fla., Gainesville.

Lalande, P., et al. (2002), Observations and modeling of lightning leaders, *C. R. Phys.*, *3*, 1375–1392, doi:10.1016/S1631-0705(02)01413-5.

Lehtinen, N. G., T. F. Bell, and U. S. Inan (1999), Monte Carlo simulation of runaway MeV electron breakdown with application to red sprites and terrestrial gamma ray flashes, *J. Geophys. Res.*, *104*, 24,699–24,712, doi:10.1029/1999JA900335.

McCarthy, M., and G. K. Parks (1985), Further observations of X-rays inside thunderstorms, *Geophys. Res. Lett.*, *12*, 393–396, doi:10.1029/GL012i006p00393.

Moore, C. B., K. B. Eack, G. D. Aulich, and W. Rison (2001), Energetic radiation associated with lightning stepped-leaders, *Geophys. Res. Lett.*, *28*, 2141–2144, doi:10.1029/2001GL013140.

Moss, G. D., V. P. Pasko, N. Liu, and G. Veronis (2006), Monte Carlo model for analysis of thermal runaway electrons in streamer tips in transient luminous events and streamer zones of lightning leaders, *J. Geophys. Res.*, *111*, A02307, doi:10.1029/2005JA011350.

Nemiroff, R. J., J. T. Bonnell, and J. P. Norris (1997), Temporal and spectral characteristics of terrestrial gamma flashes, *J. Geophys. Res.*, *102*, 9659–9665, doi:10.1029/96JA03107.

Olsen, R. C., III, V. A. Rakov, D. M. Jordan, J. Jerauld, M. A. Uman, and K. J. Rambo (2006), Leader/return-stroke-like processes in the initial stage of rocket-triggered lightning, *J. Geophys. Res.*, *111*, D13202, doi:10.1029/2005JD006790.

Parks, G. K., B. H. Mauk, R. Spiger, and J. Chin (1981), X-ray enhancements detected during thunderstorm and lightning activities, *Geophys. Res. Lett.*, *8*, 1176–1179, doi:10.1029/GL008i011p01176.

Rakov, V. A., and M. A. Uman (2003), *Lightning Physics and Effects*, Cambridge Univ. Press, New York.

Schonland, B. F. J., and J. P. T. Viljoen (1933), On penetrating radiation from thunderclouds, *Proc. R. Soc., Ser. A*, *140*, 314–333.

Shaw, G. E. (1967), Background cosmic count increases associated with thunderstorms, *J. Geophys. Res.*, *72*, 4623–4626, doi:10.1029/JZ072i018p04623.

Smith, D. M., L. I. Lopez, R. P. Lin, and C. P. Barrington-Leigh (2005), Terrestrial gamma-ray flashes observed up to 20 MeV, *Science*, *307*, 1085–1088, doi:10.1126/science.1107466.

Suszcynsky, D. M., R. Roussel-Dupré, and G. Shaw (1996), Ground-based search for X rays generated by thunderstorms and lightning, *J. Geophys. Res.*, *101*, 23,505–23,516, doi:10.1029/96JD02134.

Tsuchiya, H., et al. (2007), Detection of high-energy gamma rays from winter thunderstorms, *Phys. Rev. Lett.*, *99*, 165002, doi:10.1103/PhysRevLett.99.165002.

Wilson, C. T. R. (1925), The acceleration of beta-particles in strong electric fields such as those of thunder-clouds, *Proc. Cambridge Philos. Soc.*, *22*, 534–538, doi:10.1017/S0305004100003236.

M. Bakhtiari, Roswell Park Cancer Institute, Elm and Carlton Streets, Buffalo, NY 14263, USA.

C. Biagi, D. Hill, J. Howard, M. Stapleton, and M. Uman, Department of Electrical and Computer Engineering, University of Florida, Gainesville, FL 32611, USA.

D. Concha, Department of Earth, Atmospheric and Planetary Sciences, Massachusetts Institute of Technology, Cambridge, MA 02139, USA.

J. Dwyer, H. Rassoul, and Z. Saleh, Department of Physics and Space Sciences, Florida Institute of Technology, 150 West University Boulevard, Melbourne, FL 32901, USA. (zsaleh@fit.edu)